Molecular Biology of the Cell
Vol. 9, 977–991, May 1998

Saccharomyces cerevisiae Cells with Defective Spindle Pole Body Outer Plaques Accomplish Nuclear Migration via Half-Bridge–organized Microtubules

Arndt Brachat,* John V. Kilmartin,† Achim Wach,*‡ and Peter Philippsen*§

*Lehrstuhl für Angewandte Mikrobiologie, Biozentrum, Universität Basel, CH-4056 Basel, Switzerland; and †Medical Research Council Laboratory of Molecular Biology, Cambridge CB2 2QH, United Kingdom

Submitted December 29, 1997; Accepted February 5, 1998
Monitoring Editor: Tim Stearns

Cnm67p, a novel yeast protein, localizes to the microtubule organizing center, the spindle pole body (SPB). Deletion of *CNM67* (*YNL225c*) frequently results in spindle misorientation and impaired nuclear migration, leading to the generation of bi- and multinucleated cells (40%). Electron microscopy indicated that *CNM67* is required for proper formation of the SPB outer plaque, a structure that nucleates cytoplasmic (astral) microtubules. Interestingly, cytoplasmic microtubules that are essential for spindle orientation and nuclear migration are still present in cnm67Δ1 cells that lack a detectable outer plaque. These microtubules are attached to the SPB half- bridge throughout the cell cycle. This interaction presumably allows for low-efficiency nuclear migration and thus provides a rescue mechanism in the absence of a functional outer plaque. Although *CNM67* is not strictly required for mitosis, it is essential for sporulation. Time-lapse microscopy of *cnm67Δ1* cells with green fluorescent protein (GFP)-labeled nuclei indicated that *CNM67* is dispensable for nuclear migration (congression) and nuclear fusion during conjugation. This is in agreement with previous data, indicating that cytoplasmic microtubules are organized by the half-bridge during mating.

INTRODUCTION

Faithful segregation of duplicated nuclei is crucial for the precise propagation of genetic material in all eukaryotic cells. In the budding yeast *Saccharomyces cerevisiae*, nuclear migration comprises two major steps during the mitotic cycle. During the first step, the nucleus moves from a random position in the mother cell to a site close to the bud neck. Insertion of the elongating and separating nucleus into the daughter cell during anaphase marks the second step (Yeh *et al.*, 1995; Cottingham and Hoyt, 1997; DeZwaan *et al.*, 1997). Nuclear migration and positioning of the mitotic spindle relative to the mother–daughter axis are strictly dependent on the dynamic action of cytoplasmic (astral) microtubules (Carminati and Stearns, 1997; Shaw *et al.*, 1997). Tubulin mutants affecting predominantly cytoplasmic microtubules thus drastically impair orientation of the spindle and nuclear migration, leading to abnormal nuclear division within mother cells (Huffaker *et al.*, 1988; Sullivan and Huffaker, 1992). As a result, these mother cells accumulate two or more nuclei, whereas daughter cells lack chromosomal DNA. Other proteins required for correct segregation of nuclei include the microtubule-based motor dynein as well as putative components of the dynactin complex and the actin cytoskeleton (Magdolen *et al.*, 1988; Haarer *et al.*, 1990; Palmer *et al.*, 1992; Eshel *et al.*, 1993; Li *et al.*, 1993; Clark and Meyer, 1994; McMillan and Tatchell, 1994; Muhua *et al.*, 1994; Yeh *et al.*, 1995). Recent evidence suggests that several microtubule-based motors act in concert to achieve proper spindle positioning and nuclear migration (Cottingham and Hoyt, 1997; DeZwaan *et al.*, 1997).

Polymerization of microtubules is generally nucleated by microtubule- organizing centers (MTOCs). Al-

‡ Current address: Bureco Corp., CH-4310 Rheinfelden, Switzerland.
§ Corresponding author.

though they are morphologically diverse, MTOCs of different organisms serve similar functions in controlling the number, direction, and polarity of attached microtubules (Brinkley, 1985; Kellogg *et al*., 1994; Kalt and Schliwa, 1996; Pereira and Schiebel, 1997). The MTOC of *S. cerevisiae* is the spindle pole body (SPB), a multilayered organelle embedded in the nuclear envelope (Byers, 1981; Rose *et al*., 1993; Winey and Byers, 1993; Kilmartin, 1994; Snyder, 1994; Bullitt *et al*., 1997). A central electron-dense layer, the central plaque, lies in the plane of the nuclear membrane. On one side of the central plaque is the half-bridge, which early in G_1 has a spherical structure called the satellite attached to its cytoplasmic side. This is probably the precursor of the nascent SPB. After duplication the two SPBs are connected by fused half-bridges (now forming the bridge). Three SPB substructures are directly involved in the binding of different sets of microtubules. Intranuclear microtubules are organized by the inner plaque throughout the cell cycle. Cytoplasmic microtubules are initiated by the half-bridge or bridge during the early part of the cell cycle before SPB duplication and continuing until SPB separation. After that and for the rest of the cell cycle, they attach to the outer plaque (Byers and Goetsch, 1975). The mechanism and cellular function of the change in attachment sites for cytoplasmic microtubules are currently not understood.

Nucleation of microtubules at the outer and inner plaque is probably mediated by a protein complex containing the 90-kDa SPB component Spc98p in addition to Tub4p and Spc97p (Rout and Kilmartin, 1990; Sobel and Snyder, 1995; Geissler *et al*., 1996; Marschall *et al*., 1996; Spang *et al*., 1996; Knop *et al*., 1997). Despite the presence of this complex at both the inner and outer plaque, it seems likely that there are differences in the protein composition of these plaques since electron microscopy reveals structural differences between them. The proteins responsible for this variance remain to be elucidated.

In addition to its essential mitotic functions in spindle formation, chromosome movement, and nuclear migration, the SPB also has key roles in conjugation and sporulation. During mating, the SPBs of fusing haploid cells are connected by cytoplasmic microtubules organized by half-bridges, and nuclear fusion appears to be initiated by fusion of the two SPBs (Byers and Goetsch, 1975). In sporulating yeast cells, spore wall formation is started by an enlargement of the outer plaque, which serves as a nucleation site for spore wall assembly (Moens and Rapport, 1971; Byers, 1981).

In this paper we describe the characterization of a novel gene that is important for spindle orientation and nuclear migration. We propose the name *CNM67* (chaotic nuclear migration) since deletion of the gene results in a severe nuclear migration defect and because the gene product was also identified as a 67-kDa protein by mass spectrometric analysis of isolated yeast spindle poles (Jensen, unpublished data). Tagging of Cnm67p demonstrates its localization to the SPB region. We find by electron microscopy that the SPB outer plaque is considerably reduced in *cnm67Δ1* cells, indicating a role for Cnm67p in outer plaque formation. Cytoplasmic microtubules are apparently nucleated by the half-bridge throughout the cell cycle, thus providing a rescue pathway for spindle orientation and nuclear migration that does not depend on outer plaque-bound microtubules.

MATERIALS AND METHODS

Strains, Media, and Yeast Transformation

Yeast strains that were used in this study are summarized in Table 2. Yeast media were prepared as described by Guthrie and Fink (1991). The yeast transformation procedure was based on the protocol by Schiestl and Gietz (1989). After the heat shock step, cells were pelleted and resuspended in 5 ml of YPD and incubated for 2 h at 30°C. Cells were again pelleted, resuspended in 1 ml dH_2O, and plated on selective YPD-G418 medium (200 mg G418/l). The *Escherichia coli* strain XL1-blue (Bullock *et al*., 1987) was used to propagate plasmids.

DNA Manipulations and Strain Constructions

Standard DNA manipulations were performed as described by Sambrook *et al*. (1989). We applied a PCR-based method to construct gene deletion cassettes that were used in yeast transformations (McElver and Weber, 1992; Baudin *et al*., 1993, Wach *et al*., 1994). DNA of *E. coli* plasmids pFA6-kanMX4 (Wach *et al*., 1994) or pFA6-HIS3 MX6 (Wach *et al*., 1997) served as template for preparative PCR reactions. Oligonucleotides 5′-GGCACTAGTATGCTTGATCCGTAAATTTCTTTAGATTCATTCATCGATGAATTCGAGCTC-3′ and 5′-GCGCAGCTGATTTCGATTTAATGAATTTTCCATTTCATGAGCCGTACGCTGCAGGTCGAC-3′ were used as primers to produce *CNM67* gene deletion cassettes that replaced codons 14–537 of the gene upon integration into the genome. During a systematic analysis of novel gene functions, we constructed several GFP fusions to the 3′-ends of open-reading frames (ORFs) of unknown function (Brachat, Duesterhoeft, Moestl, Rebischung, Wach, and Philippsen, unpublished data). For amplification of GFP gene fusion constructs, the template DNA was pFA6-GFP-kanMX6 (Wach *et al*., 1997). We utilized oligonucleotide primers that introduced short flanking regions of homology to the gene's 3′-end. The PCR product was then integrated into the genome at the 3′-end of the gene by homologous recombination, creating a fusion gene that excluded the gene's stop codon. The fusion gene was thus expressed from the original promoter, minimizing the risk of non–wild-type expression levels. Primers 5′-CTGGACCATCTGTATGATCATATCCTGGAGAAGATGGTGAAGGGTCGACGGATCCCCGGG-3′ and 5′-TATACATACTTCCTAGAATATAATTTAATCTTATACCTTAACATCGATGAATTCGAGCTCG-3′ were used for generation of GFP-kanMX6 with flanking homology to the 3′-end of *CNM67*. Correct genomic integration of the corresponding construct was verified by analytical PCR (Huxley *et al*., 1990; Wach *et al*., 1994). To facilitate the production of 3HA epitope fusions to protein C termini, a pFA-3HA-kanMX6 plasmid was constructed. The 3HA antigen was amplified by PCR with primers 5′-GCGTTAATTAACTACCCATACGATGTTCCT-3′ and 5′-CCGGGCGCGCCGCACTGAGCAGCGTAATC-3′ and plasmid pSKIIHA1 (provided by B. Futcher) as template. The PCR product was cleaved with *Asc*I and *Pac*I and cloned into pFA6-GFP-kanMX6 from which the GFP sequence had been released by *Asc*I and *Pac*I digestion. The resulting plasmid was then

used as template for generation of a 3HA-kanMX6 gene fusion cassette to tag *CNM67*. Primers for this reaction were the same as for production of the GFP fusion cassette.

Heterozygous diploid strains expressing the *CNM67-GFP* or *CNM67–3HA* fusion genes were sporulated and analyzed by tetrad dissection. Cells carrying only the gene fusion allele and no wild-type copy of *CNM67* grew at the same rate as the corresponding wild-type cells. Microscopic observation of DAPI-stained cells also did not reveal any morphological or nuclear migration defects caused by the Cnm67-GFPp or Cnm67-HAp fusion protein. We used strain ABY112 to characterize the Cnm67-GFPp distribution pattern and strain ABY132 for the Cnm67-HAp pattern.

C-terminal fusion of GFPp to Hhf2p was performed as described by Wach *et al*. (1997) and caused a slight reduction in growth rates of haploid strains compared with the wild-type, but this was considered as acceptable since both strains that were to be compared in mating experiments carried the same Hhf2-GFPp label. Thus, defects visible in labeled *cnm67Δ1* but not in labeled *CNM67* cells should be specifically caused by the *cnm67Δ1* mutation. Hhf2-GFPp fluorescence produced a bright nuclear staining that proved to be very suitable for *in vivo* studies. The major advantage of this label was the fact that very short excitation times (0.12 s) could be used to obtain strong GFP fluorescence. This, in turn, drastically reduced light-induced damage to the cells and allowed for observation of cells over many generations.

Yeast strains were grown on YPD-geneticin (200 μg geneticin/ml) to select for transformants that had integrated kanMX4-, GFP-kanMX6-, or 3HA-kanMX6-derived constructs. Growth on SD plates lacking histidine selected for HIS3 MX6 integration.

We first produced a diploid homozygous *cnm67Δ1* strain by crossing haploid *cnm67Δ1* strains ABY102 and ABY103 with selection on SD medium lacking tryptophan and histidine. To obtain independent evidence for the sporulation deficiency of *cnm67Δ1* mutants in a second strain background, we constructed a diploid CEN.PK2 derivative with two deleted CNM67 alleles by two successive PCR-based gene deletions. The first allele was deleted by integration of a kanMX4 marker cassette at the *CNM67* locus. The resulting heterozygous strain was then used for transformation with a second PCR-amplified HIS3 MX6 marker cassette that carried the respective *CNM67* homology regions and rendered transformed cells His^+. Colonies that were His^+ and also still G418 (geneticin) resistant were subjected to analytical PCR for verification of both deletion alleles (ABY108). Positive clones were then incubated under sporulation conditions.

For complementation analysis of a *cnm67Δ1* strain, we subcloned a *2.4 kb Hin*dIII restriction fragment from a chromosome XIV cosmid clone into the *Hin*dIII site of pRS 416 (Sikorski and Hieter, 1989), a single-copy vector with the URA3 gene as selectable marker. The subclone plasmid (pYCGNL225c) included the complete *CNM67* coding sequence plus 218 base pairs (bp) upstream of the *CNM67* start codon and 361 bp downstream of the stop codon. The *CNM67* 3′-region included the first 23 N-terminal codons of ORF *YNL227c*, whereas the 5′-region did not include any predicted coding sequences. After transformation of haploid strain (ABY104) with the plasmid, we compared growth of the resulting Ura^+ strain (ABY106) and the corresponding wild-type strain on YPD at 30°C (Figure 1D).

Test for Benomyl Sensitivity and Synthetic Lethality

Sensitivity to benomyl on solid YPD was assayed as described by Interthal *et al*. (1995). Cells from exponentially growing CEN.PK2 and ABY108 cultures were spotted as serial dilutions onto plates containing increasing concentrations of benomyl (5–50 μg/ml). Plates were incubated at 30°C.

Double-mutant strains were constructed by *CNM67* replacement in the corresponding mutant strain background by a PCR-generated kanMX4 cassette as described above. Nuclear migration mutant strains were DBY2023 (*tub2–401*), DBY1384 (*tub2–104*), YJC1371 (*act5Δ/act5 Δ*), and *5105* (*act1–4/act1–4*). If the original nuclear migration mutant was temperature sensitive, we incubated the double mutant at a temperature very close to the restrictive temperature to test for a synthetic aggravation of defects by the *cnm67Δ,mdul1* deletion. To test for synthetic lethality, we incubated the tub2–401, *cnm67Δ1* strain at 20°C, a temperature at which the cold- sensitive *tub2–401* strain was barely able to grow (Sullivan and Huffaker, 1992). *tub2–104* (Thomas *et al*., 1985; Huffaker *et al*., 1988) was also tested for synthetic lethality with *cnm67Δ1* at the permissive temperature of 16°C. We also introduced the *cnm67Δ1* deletion in a homozygous act1–4 (Palmer *et al*., 1992) background and sporulated the resulting heterozygous *cnm67Δ1/CNM67*, *act1–4/act1–4* strain. Incubation of derived haploid double mutants was on YPD medium at 30°C or 33°C. A *cnm67Δ1/act5Δ* double-mutant strain was also constructed by *CNM67* deletion in a homozygous diploid *act5Δ* strain (Muhua *et al*., 1994) and subsequent sporulation followed by tetrad analysis and incubation on YPD at 30°C.

Fluorescence Microscopy and Electron Microscopy (EM)

For DAPI staining, yeast cells were grown in YPD to early log phase. Approximately 5×10^7 cells were pelleted, resuspended in 50 μl dH_2O, and fixed for 5 min by addition of 1 ml 70% ethanol before DAPI staining. One microliter of a 1 mg/ml DAPI stock solution was added, and the suspension was incubated for 5 min at room temperature. Cells were subsequently washed twice in dH_2O and mounted on a poly-L-lysine-treated slide for microscopy. If DAPI staining was performed for quantification of nuclear distribution, cells were first digested with Zymolyase 100T (250 μg/ml in 40 mM KH_2PO_4, pH 6.5, 1.2 M sorbitol) for 1 h at 37°C. Four microliters of the 1 mg/ml DAPI stock solution were directly added per 1 ml of the growth medium if DAPI and GFP fluorescence were to be observed in the same cells.

Immunofluorescence staining of strains ABY108, ABY132, and CEN.PK2 was performed essentially as described by Kilmartin *et al*. (1993). Fixation was for 20 min for tubulin staining and 1.5 min for hemagglutinin antigen (HA)-tubulin double staining. Cells were incubated with either rabbit anti-yeast tubulin immunoglobulin G and/or with mouse monoclonal 12CA5 anti-HA antibody overnight at 4°C. Anti-tubulin primary antibody was detected with Texas-Red–labeled goat anti-rabbit immunoglobulin G. Anti-HA–treated cells were further incubated with fluorescein-labeled anti-mouse antibody.

Fixation and embedding of mutant and wild-type cells for serial thin section electron microscopy was performed as described by Byers and Goetsch (1991) with slight modifications (Goh and Kilmartin, 1993). CEN.PK2 was used as the wild-type control and ABY108 as *cnm67Δ1* mutant strain for EM analysis.

In Vivo Time-Lapse Microscopy

Mutant or wild-type Hhf2-GFPp labeled a and α strains (DHY2, DHY3, ABY134, ABY135) were grown overnight in YPD medium to early logarithmic phase. Approximately 1×10^5 cells of the corresponding a and α strains were mixed in a glass reaction tube and incubated without shaking for 1.5 h at 30°C. One milliliter of that culture was then transferred to a 1.5-ml reaction tube and centrifuged for 5 s to sediment the cells. Most of the supernatant was discarded, leaving approximately 20 μl of cell suspension in the tube. Three microliters of this suspension were then placed on top of the agarose surface of a ground well microscopy slide (Huber & Co., Reinach, Switzerland). This had been prepared by placing a drop of growth medium (SD complete medium plus 1.7% agarose) onto the slide and covering it with a coverslip to give a planar agarose surface. The coverslip was then removed, and cells were placed on top and covered by another coverslip that was sealed with nail hardener to allow for long investigation times without liquid loss.

GFP fluorescence could then be followed for more than 10 h without significant loss of intensity when very short excitation times were used and excitation was repeated only every 3 or every 5 min. Fluorescence pictures were captured and stored electronically. Fluorescence excitation was controlled by a shutter controller in combination with a MAC2000 shutter system (Ludl controller MAC 2000, Ludl Electronics, Hawthorne, NY). We used a VI-470 video camera and controller (Optronics Engineering, Goleta, CA) for picture taking.

Computer Programs and Hardware

We used the following computer programs for sequence analysis: FASTA (Pearson and Lipman, 1988) (word size = 2), PERCOIL (Berger *et al.*, 1995) with default parameters (probability cutoff = 0.5), ISOELECTRIC (Genetics Computer Group program package [1991]). Image acquisition and processing for fluorescence microscopy was performed on a Power Macintosh 7600/120 computer using the public domain NIH image 1.60 program (developed by Wayne Rasband at the US National Institutes of Health and available from the Internet by anonymous FTP from zippy.nimh.nih.gov or on floppy disk from the National Technical Information Service, Springfield, VA, part number PB95–500195GEI). Picture files were eventually contrast enhanced using Photoshop 4.0 (Adobe Systems Europe, Edinburgh, Scotland). Custom macros were used to control the microscope, the video camera, the MAC2000, and a LG-3 framegrabber (Scion, Frederick, MD).

RESULTS

CNM67 Encodes a Novel Putative Coiled-Coil Protein That Localizes to the SPB

Originally, *CNM67* (YNL225c) was identified as one of the novel ORFs on chromosome XIV of *S. cerevisiae* during systematic sequencing (Philippsen *et al.*, 1997). To analyze the subcellular localization of gene products of such novel ORFs, we used PCR targeting (Wach *et al.*, 1997) to construct genomic GFP fusions that were expressed from the original ORF promoters.

In vivo fluorescence microscopy detected Cnm67-GFPp staining as either one or two intense spots at the nuclear periphery (Figure 1A), suggesting localization to the SPB region. Unbudded cells usually contained one spot, whereas cells with intermediate sized buds showed two spots close to the DAPI- stained region of the nucleus. The maximal distance between them was never greater than the diameter of a nucleus. Large budded cells with elongating nuclei contained one spot at either pole of the DAPI-stained region, consistent with a localization to the poles of an anaphase B spindle. This result was confirmed by an independent experiment in which we constructed a *CNM67*-3HA fusion gene. Cnm67–3HAp cells were double stained with anti-HA and anti-tubulin antibodies (Figure 1B). HA staining was very similar to the Cnm67-GFPp fluorescence pattern and was always found at the poles of mitotic spindles. Cnm67-GFPp and Cnm67–3HAp fusion proteins were functional because corresponding cells carrying the fusion allele and lacking the wild-type allele showed none of the phenotypes associated with *CNM67* deletion (see below). Thus, the observed GFP- or immunofluorescence pattern of these constructs should reflect the wild-type localization of Cnm67p, and we conclude that Cnm67p is either a central component of the yeast SPB or closely associated to the SPB.

Analysis of the presumptive 581-amino acid sequence of Cnm67p with the Paircoil program (Berger *et al.*, 1995) suggests the presence of three separate coiled-coil–forming regions (see Figure 2A). Cnm67p may therefore stabilize a homo-oligomer or a complex with other proteins via a central coiled-coil region.

Comparison of the predicted Cnm67p amino acid sequence with sequences in the EMBL and PIR databases did not detect proteins of high homology. The highest FASTA (Pearson and Lipman, 1988) scores were found for other coiled-coil proteins and probably only reflected a structural similarity of the respective coiled-coil regions.

The Role of CNM67 in Nuclear Migration and Sporulation

A complete deletion of *CNM67* was found to be viable but resulted in a slow-growth phenotype (Figure 2B). When *CNM67*-deleted cells were stained with DAPI, a severe nuclear migration defect was observed (Figure 3). Table 1 summarizes the frequency of abnormal distribution of nuclei in ABY108, a homozygous diploid *cnm67Δ1* deletion strain. Many mother cells (26%) contained two separated chromosome masses, indicating a completion of nuclear division without migrating the daughter nucleus to the bud; 14% of the cells even showed three to eight nuclei and about 5% carried no nucleus. Some of the bi- or multinucleated cells also displayed morphological defects. Although a substantial portion of cells showed pronounced defects, we also observed many cells (56%) with a single nucleus, suggesting the presence of a protein with an overlapping function to that of Cnm67p or correct alignment of the nuclei occurring by chance. The slow growth behavior, nuclear migration defect, and impaired morphogenesis were found for haploid and homozygous diploid *cnm67Δ1* cells derived from two different genetic backgrounds (*ABY99, ABY102, ABY103, ABY104, ABY107, ABY108* in Table 2). Time-lapse analysis of *cnm67Δ1* cells with GFP-labeled nuclei by fluorescence microscopy suggested that misorientation of the mitotic spindle was the primary defect whereas morphological abnormalities were later consequences of *CNM67* loss (Hoepfner, personal communication).

To test for complementation of the observed defects, we transformed *cnm67Δ1* cells with a plasmid containing the *CNM67* wild-type allele. The resulting transformants grew at the same rate as the corresponding wild-type strain (Figure 2C), and fluorescence microscopy of DAPI-stained cells showed wild-type distri-

Table 1. Nuclear migration in diploid *cnm67Δ1* (ABY108)- and wild-type (CEN.PK2) strains

		Nuclear migration phenotype				
	Yeast strain	0 Nucleus per cell	1 Nucleus per cell	2 Nuclei per cell	3 Nuclei per cell	>3 Nuclei per cell
16°C	*CNM67*	0 %	99.6%	0.4%	0 %	0 %
	cnm67Δ1	4.4%	57.5%	25.3%	7 %	5.8%
30°C	*CNM67*	0 %	98 %	2 %	0 %	0 %
	cnm67Δ1	4.9%	55.6%	25.7%	6.6%	7.2%
37°C	*CNM67*	0.1%	99.5%	0.4%	0 %	0 %
	cnm67Δ1	8.3%	52.3%	32.2%	5.7%	1.5%

The number of nuclei per cell in diploid yeast strains was determined by DAPI staining of asynchronous cultures in exponential growth phase. Greater than 500 cells were counted for each strain. Cells of different morphologies were grouped according to their nuclear distribution as indicated at the top.

bution of nuclei. We conclude that the *CNM67* clone fully complemented the *cnm67Δ1* defects, and thus the observed defects in cnm67Δ1 strains were due to deletion of the *CNM67* gene.

We also investigated the sporulation efficiency of a homozygous diploid *cnm67Δ1* strain. The wild-type control strain *(CEN.PK2)* sporulated efficiently (70% four spored asci after 5 d on sporulation medium) whereas we did not observe asci with spores among more than 400 *cnm67Δ1* cells *(ABY108)*. Even after several weeks on sporulation plates, no asci were visible, indicating that the *CNM67* gene is essential for sporulation. This result was further confirmed with another homozygous *cnm67Δ1* deletion strain of different genetic background *(ABY107)*.

Characterization of the Microtubule Cytoskeleton of cnm67Δ1 Cells

Immunofluorescence staining of tubulin in *cnm67Δ1* cells revealed several defects in microtubule structure (Figure 3). In large budded cells, spindle microtubules that connected two chromosome masses were frequently restricted to the mother cell without penetrating the bud neck (Figure 3B1). Among these cells some had aligned the spindle along the mother–bud axis, whereas in others the spindles were oriented randomly relative to this axis. Many cells clearly showed cytoplasmic microtubules directing into the bud (Figure 3B, 1 and 2). Multinucleated cells frequently contained spindles that crossed over one another (Figure 3B3), indicating independent orientation of spindles relative to each other within one cell. Elongation of spindles usually appeared to be synchronized in cells that contained more than one nucleus, suggesting that the coupling of spindle dynamics to the general control of cell cycle progression was still functional (Adams and Pringle, 1984; Kilmartin and Adams, 1984). The length of some spindles drastically exceeded the diameter of the mother cell, leading to bent spindles (Figure 3B1), which was probably due to a continued spindle elongation without accompanying migration of the spindle toward the daughter cell. This could also be seen in mother cells containing a spindle that was oriented along the mother–bud axis, suggesting that pushing forces of an elongating spindle were not sufficient to drive effective penetration of the spindle through the bud neck. In other *cnm67Δ1* cells, several DAPI- stained regions appeared to be connected by microtubules. Here, we could not definitely distinguish between a cytoplasmic or nuclear origin of these microtubular structures. A clear quantitative description of frequencies of different microtubular structures in *cnm67Δ1* cells was made impossible by the extreme heterogeneity of spindle morphologies and numbers. We suppose that the observed defect in nuclear migration is a consequence of spindle misorientation in combination with inefficient pulling of the spindle through the bud neck.

Test for Benomyl Sensitivity and Synthetic Lethality with Nuclear Migration Mutants

Mutations in tubulin-interacting proteins or in tubulin itself often cause an altered sensitivity to the microtubule-destabilizing drug benomyl (Thomas *et al*., 1985; Stearns *et al*., 1990; Solomon, 1991; Interthal *et al*., 1995). Since Cnm67p is involved in the microtubule-dependent process of nuclear migration, we tested the benomyl tolerance of a *cnm67Δ1* strain by spotting serial dilutions of cells onto plates with increasing concentrations of benomyl. We did not observe any significant difference between the sensitivity of the *cnm67Δ1* strain and the isogenic wild-type strain. Growth of both strains on solid YPD medium at 30°C was completely inhibited at benomyl concentrations >20 μg/ml.

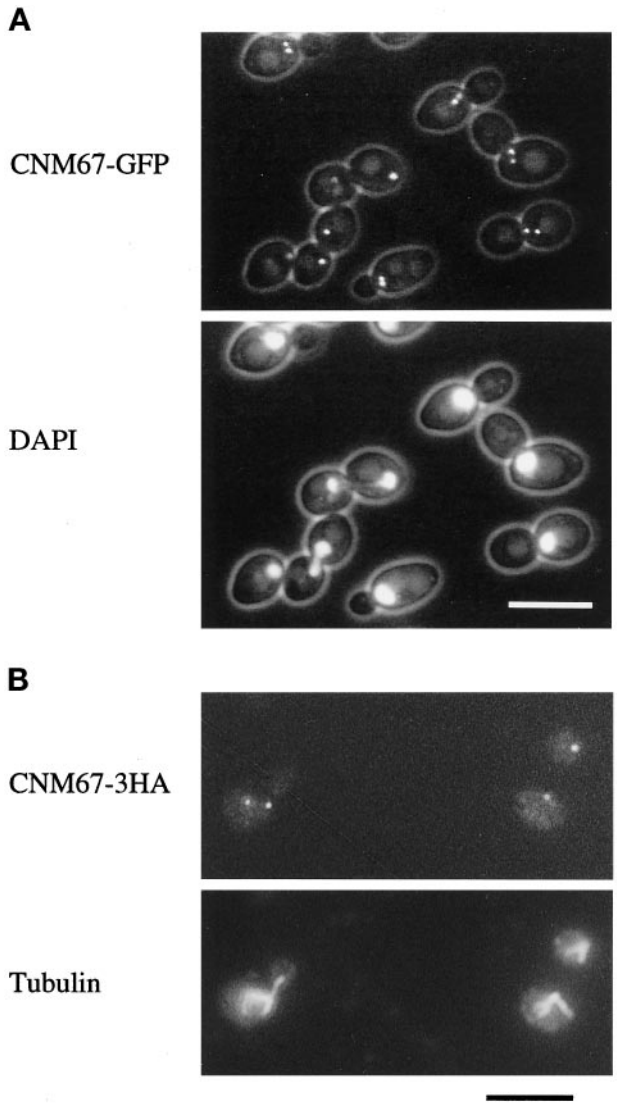

Figure 1. Subcellular localization of functional Cnm67p fusion proteins visualized by fluorescence microscopy. (A) Cnm67-GFPp fluorescence is visible at one or two spots at the nuclear periphery, consistent with a localization to the SPB. Nuclear DNA was stained with DAPI. (B) Immunofluorescence microscopy of Cnm67–3HAp–labeled cells. Dot-shaped staining with anti-HA antibody coincides with the spindle poles visualized by tubulin staining with anti-tubulin antibody.

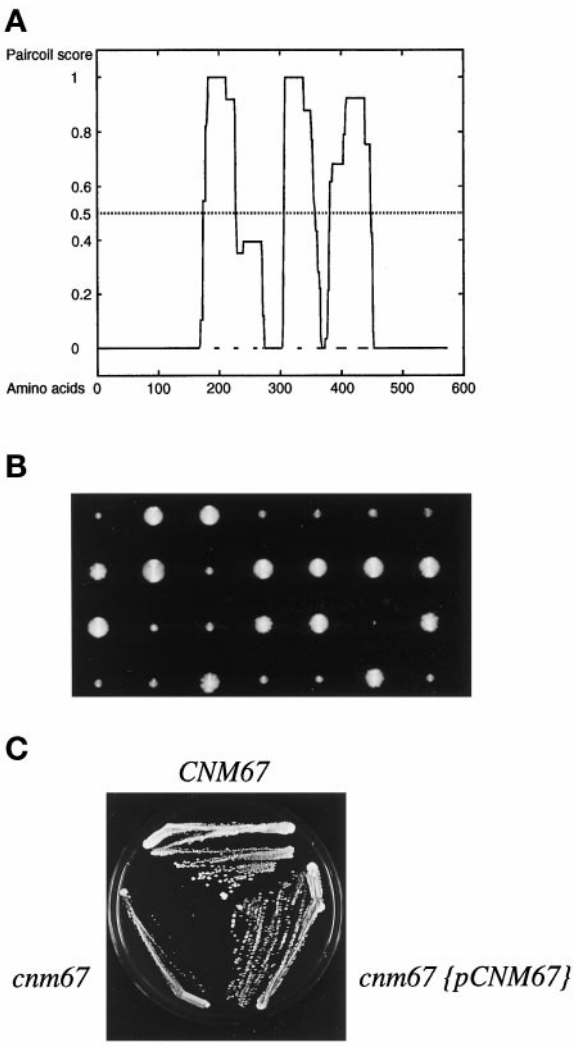

Figure 2. Cnm67p coiled-coil prediction, tetrad analysis, and complementation test. (A) Probability plot for coiled-coil formation of the 581 amino-acid sequence of Cnm67p. The central part of the protein was predicted to contain three α helical coiled-coil regions (residues 174–226, p = 1; residues 306–357, p = 1; residues 382–448, p = 0.924) by the Paircoil program (Berger *et al.*, 1995). The *CNM67* sequence is available from EMBL/GenBank/DDBJ under accession number Z71501. (B) Tetrad dissection of a heterozygous *CNM67*-deleted strain (ABY101). Tetrad colonies were transferred on G418 containing medium to test for segregation of the *kanMX4* gene deletion marker. Slow growing colonies always carried the *cnm67::kanMX4* allele (*cnm67Δ1*). (C) Complementation of the *cnm67Δ1* growth defect by transformation with a plasmid carrying the *CNM67* wild-type allele.

A number of mutants that influence the fidelity of spindle orientation and nuclear movement during mitosis are known. To search for genetic interactions of *CNM67*, we tested synthetic lethality of the *CNM67* deletion with the nuclear migration mutants *tub2–401, tub2–104, act5*, or *act1–4* (Huffaker *et al.*, 1988; Sullivan and Huffaker, 1992; Clark and Meyer, 1994; Muhua *et al.*, 1994; Palmer *et al.*, 1992). None of the tested double mutants resulted in a synthetic lethal phenotype.

SPB Ultrastructure of cnm67Δ1 Cells

Impaired nuclear migration of *cnm67Δ1* cells in combination with the localization of Cnm67p to the SPB pointed to a role of Cnm67p at the SPB substructures that organize the attachment of cytoplasmic microtubules. We investigated more than 300 SPBs of *cnm67Δ1* cells by serial thin section EM to determine

Table 2. Yeast strains

Name	Genotype	Source or reference
FY1679	*MATα/a ura3-52/ura3-52 trp1Δ63/TRP1 leu2Δ1/LEU2 his3Δ200/HIS3*	B. Dujon, diploid from cross FY23 × FY73 (F. Winston)
CEN.PK2	*MATα/a ura3-52/ura3-52 trp1-289/trp1-289 leu2-3,112/leu2-3,112 his3Δ1/his3Δ1*	K.D. Entian
ABY99	*MATα cnm67Δ1::kanMX4 ura3-52 trp1-289 leu2-3,112 his3Δ1*	Brachat *et al.*[a]
ABY101	*MATα/a cnm67Δ1::kanMX4/CNM67 ura3-52/ura3-52 trp1Δ63/TRP1 leu2Δ1/LEU2 his3Δ200/HIS3*	Brachat *et al.*[a]
ABY102	*MATα cnm67Δ1::kanMX4 ura3-52 TRP1 leu2Δ1 his3Δ200*	Brachat *et al.*[a]
ABY103	*MATa cnm67Δ1::kanMX4 ura3-52 trp1Δ63 leu2Δ1 HIS3*	Brachat *et al.*[a]
ABY104	*MATa cnm67Δ1::kanMX4 ura3-52 trp1Δ63 leu2Δ1 his3Δ200*	Brachat *et al.*[a]
ABY105	*MATα/a cnm67Δ1::kanMX4/CNM67 ura3-52/ura3-52 trp1-289/trp1-289 leu2-3, 112/leu2-3,112 his3Δ1/his3Δ1*	This study
ABY106	*MATa cnm67Δ1::kanMX4 ura3-52 trp1Δ63 leu2Δ1 his3Δ200* {pYCGNL225c}[b]	This study
ABY107	*MATα/a cnm67Δ1::kanMX4/cnm67Δ1::kanMX4 ura3-52/ura3-52 trp1Δ63/TRP1 leu2Δ1/leu2Δ1 his3Δ200/HIS3*	This study
ABY108	*MATα/a cnm67Δ1::kanMX4/cnm67Δ1::HIS3MX6 ura3-52/ura3-52 trp1-289/trp1-289 leu2-3,112/leu2-3,112 his3Δ1/his3Δ1*	This study
ABY109	*MATα/a CNM67::GFP-kanMX6/CNM67 ura3-52/ura3-52 trp1-289/trp1-289 leu2-3,112/leu2-3,112 his3Δ1/his3Δ1*	This study
ABY110	*MATα CNM67::GFP-kanMX6 ura3-52 trp1-289 leu2-3,112 his3Δ1*	This study
ABY111	*MATa CNM67::GFP-kanMX6 ura3-52 trp1-289 leu2-3,112 his3Δ1*	This study
ABY112	*MATα/a CNM67::GFP-kanMX6/CNM67::GFP-kanMX6 ura3-52/ura3-52 trp1-289/trp1-289 leu2-3,112/leu2-3,112 his3Δ1/his3Δ1*	This study
ABY132	*MATα/a CNM67::HA-kanMX6/CNM67::HA-kanMX6 ura3-52/ura3-52 trp1-289/trp1-289 leu2-3,112/leu2-3,112 his3Δ1/his3Δ1*	This study
DHY2	*MATα cnm67Δ1::kanMX4 HHF2::GFP-kanMX6 ura3-52 TRP1 leu2Δ1 his3Δ200*	This study
DHY3	*MATa cnm67Δ1::kanMX4 HHF2::GFP-kanMX6 ura3-52 trp1Δ63 LEU2 HIS3*	This study
ABY134	*MATα HHF2::GFP-kanMX6 ura3-52 trp1Δ63 HIS3 LEU2*	This study
ABY135	*MATa HHF2::GFP-kanMX6 ura3-52 TRP1 leu2Δ1 his3Δ200*	This study
5105	*MATα/a act1-4/act1-4 ura3/ura3 LEU2/leu2 HIS3/his3*	Palmer *et al.*, 1992
DBY2023	*MATa tub2-401 ura3-52 his4-539 lys2-801*	Huffaker *et al.*, 1988
DBY1384	*MATa tub2-104 ura3-52 his4-539*	Thomas *et al.*, 1985
YJC1372	*MATα/a act5Δ1::HIS3/act5Δ1::HIS3 ura3-52/ura3-52 trp1Δ63/trp1Δ63 leu2Δ1/leu2Δ1 his3Δ200/his3Δ200 lys2-801/lys2-801 ade2-101/ade2-101*	J. Cooper (Washington University)

[a] Manuscript in preparation.

[b] pYCGNL225c is a pRS416 (Sikorski and Hieter, 1989) derivative containing *CNM67* with promoter and terminator sequences.

the spindle and SPB ultrastructure (Figure 4). Wild-type SPBs clearly showed a central plaque embedded in the nuclear envelope in addition to an inner and outer plaque on the nuclear or cytoplasmic side of the nuclear membrane, respectively (Figure 4A). In contrast, the outer plaque of cnm67Δ1 cells could not be clearly visualized in any of the cells. The central and inner plaques were visible and appeared to be structurally normal (Figure 4B). Nuclear microtubules and SPB half-bridges also showed no obvious defect. These observations suggested a specific role of Cnm67p in outer plaque formation or stabilization. The prediction of Cnm67p being a coiled-coil–forming protein favors the idea of a structural role in the establishment of outer plaque integrity.

Where do cytoplasmic microtubules attach themselves in cells with a nonfunctional outer plaque? Cytoplasmic microtubules are difficult to detect by serial thin section EM of *S. cerevisiae* since there are only a few per SPB and, unlike nuclear microtubules, they emerge from the SPB at many different angles and thus rarely lie in the same plane of the section as the nuclear microtubules. Despite the apparent reduction of the SPB outer plaque, which normally initiates cytoplasmic microtubules after SPB separation, cytoplasmic microtubules were still detectable in 36 of the *cnm67Δ1* cells examined by EM. In 22 of these cells the cytoplasmic microtubules were clearly connected to the half-bridge (Figure 4, B and D), the bridge (Figure 4E), or the region between the half-bridge and the central plaque. In the remainder the microtubules ended before the SPB, and thus it was not clear what substructure they were connected to. In 10 of the 22 cells cytoplasmic microtubules originated from the bridge of side-by-side SPBs as seen in wild-type cells. However, interestingly, the connection to the half-bridge was still visible after SPB separation in 8 cells (Figure 4B). The remaining 4 cells had cytoplasmic microtubules connected to a half-bridge of a single SPB, but in three cases it was not possible to determine whether a second SPB was present in that cell. One cell (Figure 4D) presumably was in G_1 since no second

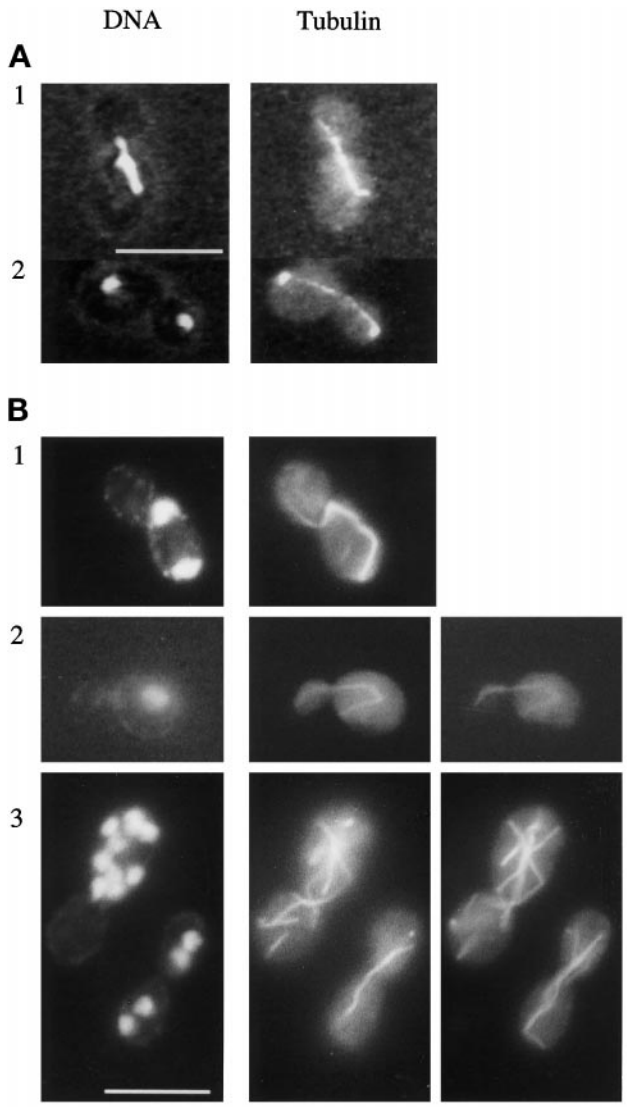

Figure 3. Nuclear distribution and microtubule structure in wild-type and *cnm67Δ1*. Cells were double stained for nuclear DNA with DAPI and for tubulin with anti-tubulin antibody. (A) Wild-type. (B) *cnm67Δ1* cells. Panels B2 and B3 show different focal planes of the respective cells to visualize the complete microtubular structures. B1 and B2 show cytoplasmic microtubules that direct from one spindle pole into the bud. The spindle in B1 is highly elongated although it is restricted to the mother cell. Panel B3 depicts multinucleated cells. Bars, 10 μm.

SPB and no bud were observed. In wild-type cells all cytoplasmic microtubules were attached to the outer plaque after SPB separation, as originally described by Byers and Goetsch (1975). It is probable that in *cnm67Δ1* cells, unlike in wild-type, cytoplasmic microtubules stay bound to the SPB half-bridge after SPB separation. In this way the mutant may partially compensate for the inability to grow cytoplasmic microtubules from the outer plaque and thus allow cells to maintain a limited nuclear migration capability. In Figure 5 our observations on spindle orientation and microtubule binding in *cnm67Δ1* cells are combined to a model for a nuclear migration-rescue mechanism that relies on half-bridge–attached microtubules.

Nuclear Fusion in cnm67Δ1 Crosses

During karyogamy, haploid nuclei migrate toward each other before they fuse their SPBs, nuclear envelopes, and nucleoplasms to produce a diploid zygote nucleus. This step was termed nuclear congression (Kurihara *et al*., 1994; Rose, 1996) and strictly depends on intact cytoplasmic microtubules that are attached to the SPB half-bridges of haploid nuclei (Byers and Goetsch, 1975; Delgado and Conde, 1984; Hasek *et al*., 1987; Rose and Fink, 1987). Our EM data indicated that *CNM67* loss considerably impairs SPB outer-plaque formation but not half-bridge structure. Hence, nuclear congression should be less impaired than mitotic nuclear migration since it relies on half-bridge–organized microtubules rather than on those that are nucleated by the outer plaque. We tested this hypothesis in two independent experiments. Initially, we examined the ability of haploid *cnm67Δ1* strains to mate by crossing an α *cnm67Δ1, his3Δ200, TRP1* and an a *cnm67Δ1, HIS3, trp1Δ63* strain. Incubation on synthetic minimal medium, lacking histidine and tryptophan, selected for diploid cells. Resulting prototroph colonies were additionally checked for diploidy by analytical PCR as described by Huxley *et al*. (1990). To confirm that prototroph colonies did not arise from heterokaryotic cells in which only cytoplasmic fusion had occurred without nuclear fusion (cytoductants), we stained the corresponding cultures with DAPI and determined the amount of mono- and multinucleated cells. We found that 60% of cells were mono- and 34% were multinucleated. Prototroph, mononucleated cells

Figure 4 (facing page). Thin section electron microscopy of wild-type and *cnm67Δ1* spindles. The nucleus is marked by 'n' and the cytoplasm by 'c'. (A) SPB of a wild-type cell with elongated spindle. The SPB half-bridge as well as the central, inner, and outer plaque of the SPB are visible. The arrowhead shows the outer plaque. Cytoplasmic microtubules do not lie within the plane of the section. (B1–2) Serial thin sections of a complete *cnm67Δ1* spindle after SPB separation. Unlike in wild-type cells, cytoplasmic microtubules are attached to the half-bridge of the upper SPB. Arrowheads show cytoplasmic microtubules and the half-bridge. (C1–2) Serial thin sections of a *cnm67Δ1* spindle. The SPB outer plaque is not detectable in any of the sections, although the half-bridge, central, and inner plaques appear normal. The same was found for all *cnm67Δ1* SPBs that we investigated *(n>300)*. (D) Cytoplasmic microtubules are attached to the half-bridge of a *cnm67Δ1* cell with a single SPB, presumably a G_1 cell. Arrowheads show the half-bridge and cytoplasmic microtubules. (E) Side- by-side SPBs are connected by a bridge that nucleates cytoplasmic microtubules directing into the bud. The bridge and cytoplasmic microtubules are indicated. Bars, 0.1 μm.

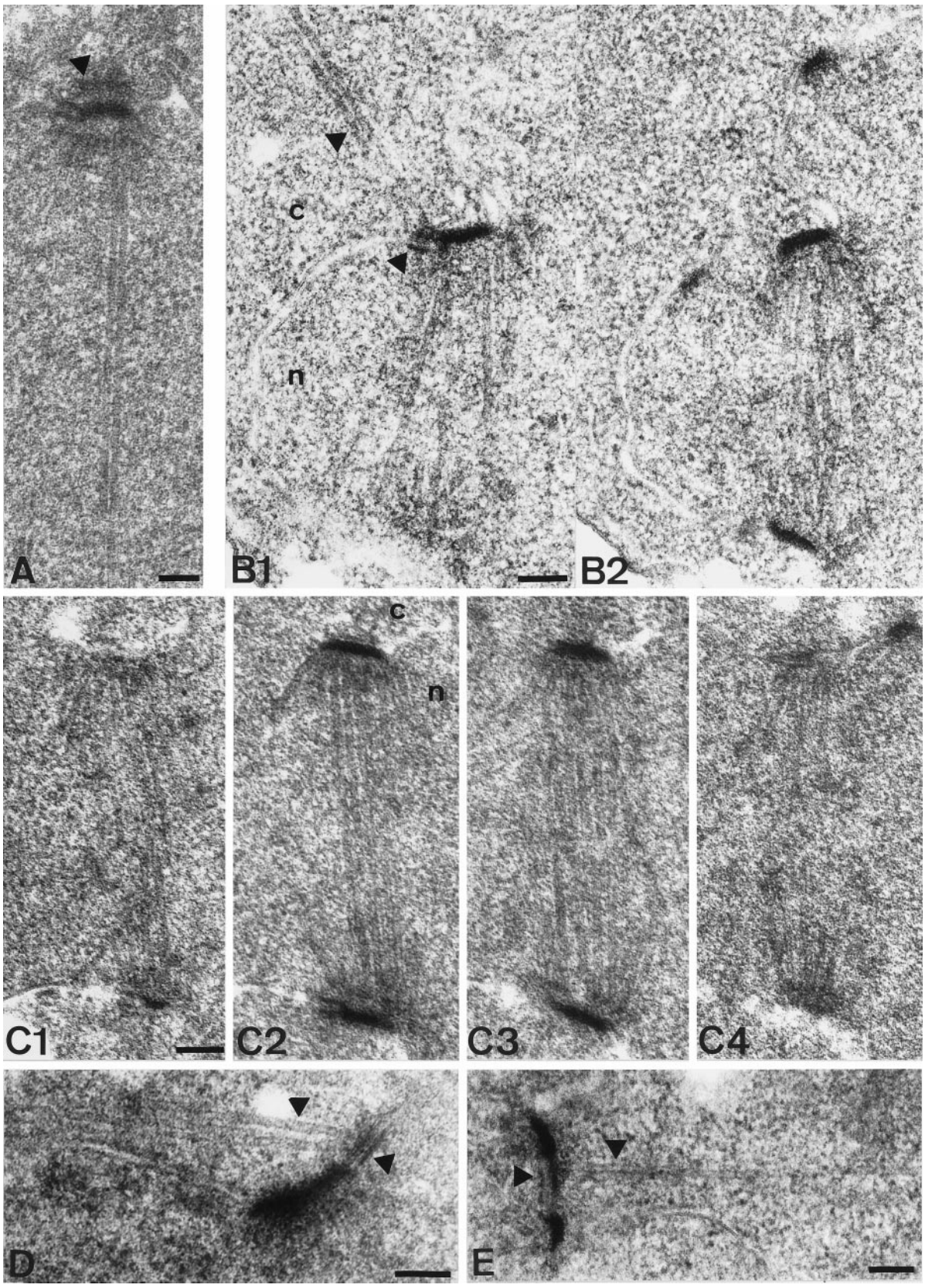

Figure 4.

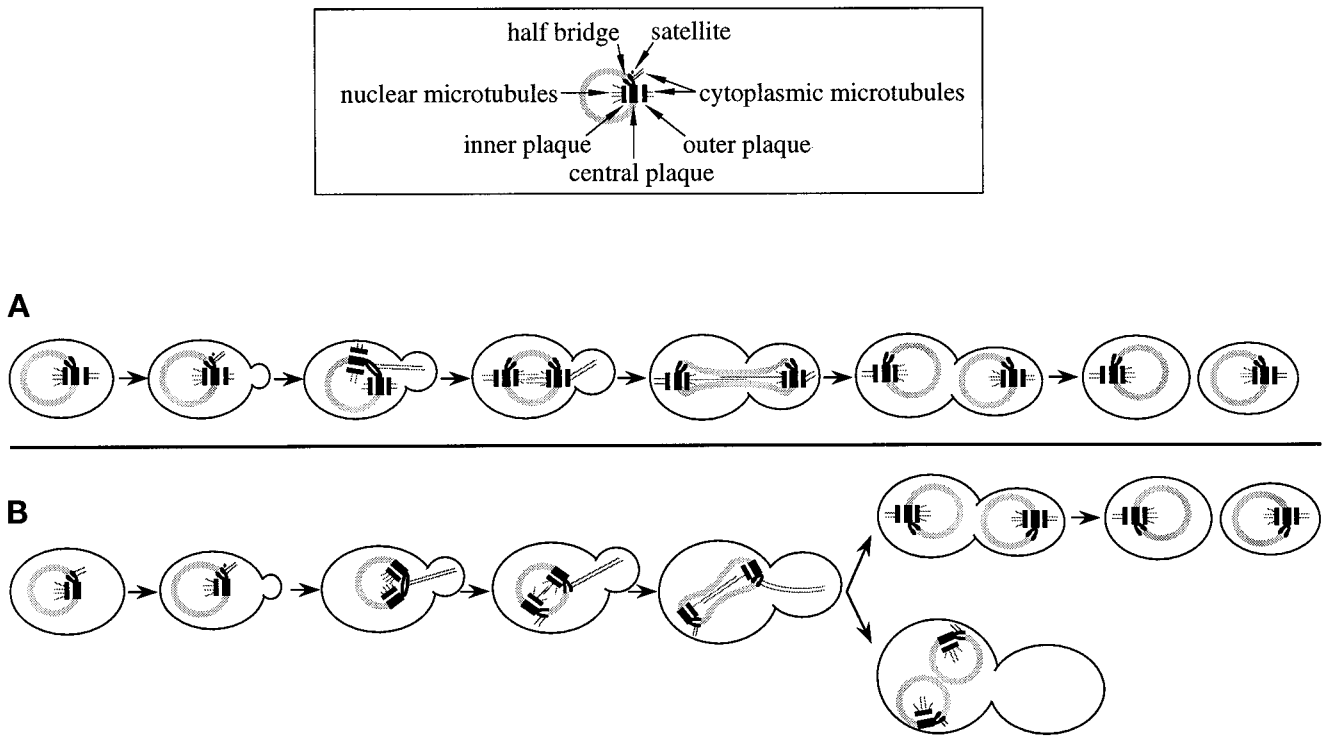

Figure 5. Model for a salvage mechanism for spindle orientation and nuclear migration in *cnm67Δ1* cells. (A) Wild-type: SPB half-bridges and bridges bind cytoplasmic microtubules only when the satellite forms and SPB duplication takes place. After SPB separation, cytoplasmic microtubules are no longer found at the half-bridge (Byers and Goetsch, 1975). During all cell cycle stages, the outer plaque acts as an attachment site. The first phase of nuclear migration begins in S when cytoplasmic microtubules originate from the bridge of side-by-side SPBs. The second phase of nuclear migration in G2/M coincides with cytoplasmic microtubule attachment at the outer plaque. (B) In *cnm67Δ1* cells cytoplasmic microtubules originate from the half-bridge throughout the cell cycle while the outer plaque is much reduced or absent and thus incapable of microtubule binding. Consequently, the second phase of nuclear migration is impaired, frequently leading to nuclear division within the mother cell. However, half-bridge–organized cytoplasmic microtubules still have a limited capability to mediate spindle positioning and nuclear migration forces that allow many cells to finally migrate the daughter nucleus into the bud. Cells in which nuclear migration failed double in ploidy and often undergo another round of nuclear division.

are presumably derivatives of haploid cells that had fused their nuclei to produce true diploids. These preliminary data suggested that *CNM67* is not required for nuclear fusion during mating.

We attempted to obtain direct evidence for the nuclear fusion capability of *cnm67Δ1* cells and to gain insight into the dynamics and efficiency of nuclear migration during conjugation and the following mitosis. For this purpose, we constructed cells with a strongly fluorescent nuclear GFP label and observed conjugating cells *in vivo* with a time-lapse video microscopy setup. Our recently described Hhf2GFPp (histone H4-GFP) fusion construct (Wach *et al*., 1997) proved to be suitable for following nuclear dynamics during the mating process and subsequent mitotic cell cycles. Figure 6A shows pictures of selected time points during mating and the first mitotic division of Hhf2-GFPp-labeled wild-type cells, and Figure 6B gives an example for a typical mating event of *cnm67Δ1* cells. Eight individual wild-type conjugation events were followed. In all cases, nuclear fusion took place as described by Cross *et al*. (1988) and Rose (1996). Nuclei moved toward each other in a directed manner and fused in the central region of the newly formed zygote. The first zygote bud developed either in the proximity of the previous cell fusion boundary or at one of the distal tips of the zygote. In any case, the nucleus reliably elongated into the zygote bud during the first mitotic division. Cytokinesis took place about 30 min after the two chromosome masses

Figure 6 (facing page). Time-lapse fluorescence video microscopy of wild-type and *cnm67Δ1* conjugations. Nuclei of haploid cells were labeled with a strongly fluorescent histone H4-GFPp (Hhf2-GFPp). (A) A nuclear fusion event of wild-type cells is followed by the first mitotic division of the zygote nucleus. Both daughter nuclei are correctly segregated between the zygote and the bud. Nuclear division is then followed by cytokinesis. (B) Conjugation of *cnm67Δ1* cells. Nuclear migration (congression) before nuclear fusion and nuclear fusion occur as in wild-type cells in the central region of the zygote and also with about the same dynamics. The subsequent mitotic division, however, fails to segregate one of the daughter

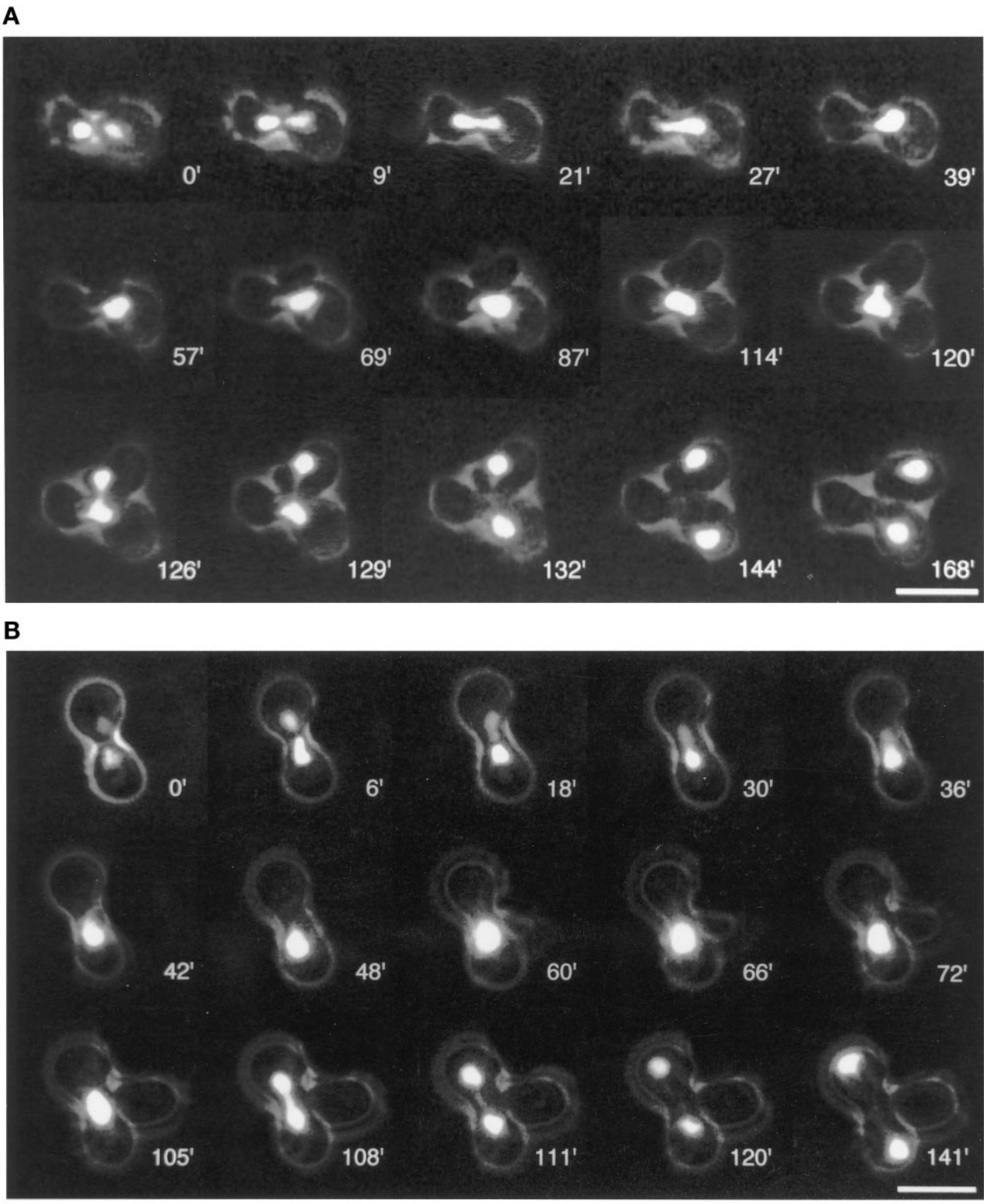

Figure 6 (cont). nuclei into the zygote bud. Presumably, congression is not affected because it is mediated by half-bridge–organized microtubules as in wild-type, whereas the first mitotic nuclear migration is impaired by the outer plaque defect of *cnm67Δ1* cells. Cells that surrounded mating cells in panels A and B were removed electronically for clarity. Bars, 10 μm.

had completely separated. Nuclear migration during following mitotic divisions also occurred reliably. We recorded 32 mating events of *cnm67Δ1* cells. Most importantly, almost all cases clearly indicated that nuclear fusion also occurs in *cnm67Δ1* zygotes. In 28 of 32 cases, both mating partners contained one nucleus before cell fusion. In 27 of these 28 cases nuclear fusion occurred with about the same dynamics as seen for the wild-type. As in wild-type cells, nuclei initially adopted a characteristic, roughly triangular, shape before they started to fuse. Presumably, this change of nuclear morphology reflected microtubule-mediated forces that acted on SPBs to pull both SPBs together, before nuclear envelope fusion. Thus, these results confirmed that *CNM67* is dispensable for the congression and nuclear envelope fusion steps of karyogamy. In one of the 28 cases mentioned above, nuclei migrated toward each other but did not fuse or show any further activity, suggesting a severe cellular malfunction that may or may not have been due to *CNM67* loss. A major difference of *cnm67Δ1* cells compared with wild-type cells became visible during the first mitotic division of newly formed diploid nuclei. In 19 of 27 cases, nuclear elongation was restricted to the zygote, without migrating the daughter nucleus into the zygote bud. The direction of nuclear elongation was usually different from the zygote–bud axis. Thus, the first mitotic division of *cnm67Δ1* zygotes was strikingly similar to divisions of vegetativly growing *cnm67Δ1* cells. Although nuclear migration before nuclear fusion was obviously unaffected, nuclear migration after nuclear fusion was heavily impaired. In 3 of 4 observable cases in which the zygote bud obtained a nucleus, nuclear division was followed by cytokinesis. Importantly, offspring of the first daughter cell clearly budded in a bipolar pattern that is typical for diploid cells (Freifelder, 1960). Those zygotes that did not succeed in migrating the nucleus into the first zygote bud often formed one or more additional buds at the distal ends of the cell. In 3 of 12 cases that could be followed, this second zygote bud obtained a nucleus. Zygotes that did not succeed in migrating daughter nuclei in buds often lysed after further nuclear divisions. Four mating events were observed in which one mating partner carried two nuclei. Nuclear fusion occurred in 3 of these 4 cases, but cells then died without dividing their nucleus.

Our data indicate that nuclear congression and envelope fusion are not significantly impaired in *cnm67Δ1* mutants. Nevertheless, the overall efficiency of mating is reduced due to defects in the segregation of diploid zygote nuclei that often lead to cell death. Fusion events between bi- or multinucleated cells also have frequently fatal consequences.

DISCUSSION

We identified and characterized *Cnm67p*, a novel yeast protein that plays a crucial role in spindle orientation and mitotic nuclear migration. DNA and tubulin staining of *CNM67* null mutants reveals the frequent misorientation of mitotic spindles, indicating that cytoplasmic forces acting on spindle poles are impaired. This deficiency then often leads to a restriction of anaphase spindle elongation to the mother cell and hence to an accumulation of nuclei in mother cells.

Interestingly, the spindle assembly checkpoint (Hoyt *et al.*, 1991; Li and Murray, 1991; Weiss and Winey, 1996) does not stop cell cycle progression in *cnm67Δ1* strains, although outer plaque structure is impaired. The most likely explanation for the failure of cell cycle arrest in *cnm67Δ1* cells is that this checkpoint does not monitor the structural integrity of the outer plaque, thus allowing the cell cycle to progress even with imperfect SPBs.

Fluorescence microscopy of cells with two independent *Cnm67p* labels showed its localization to the SPB region. This is consistent with data from mass spectrometric analysis of isolated SPBs identifying *Cnm67p* (Jensen, unpublished data). Two lines of evidence suggest a role of Cnm67p at the cytoplasmic side of the SPB. First, nuclear migration as a cytoplasmic microtubule-dependent process is heavily impaired in *cnm67Δ1* mutants, whereas nuclear microtubule-dependent processes such as SPB separation and spindle elongation are apparently normal. Second, serial thin section electron microscopy of *cnm67Δ1* cells indicates a loss of SPB outer plaque integrity while central plaque, inner plaque, half-bridge, and nuclear microtubules are indistinguishable from those of wild-type cells. A *CDC37* mutant was recently described to be defective in outer plaque formation during SPB duplication (Schutz *et al.*, 1997). Genetic data on that mutant suggest a general role of *CDC37* function in G_1 control rather than a structural role as in the case of *CNM67*. We assume that Cnm67p is a component of the outer plaque itself or a region between outer and central plaque that anchors the outer plaque to the central plaque (Bullitt *et al.*, 1997). A model that summarizes phenotypes of *cnm67Δ1* cells is shown in Figure 5.

A further defect that might be expected in a mutant with an impaired outer plaque structure is in spore wall formation, since the outer plaque serves as initiation site for spore wall assembly (Moens and Rapport, 1971; Horesh *et al.*, 1979). Our finding that *cnm67Δ1* cells are unable to sporulate is consistent with this defect, although we did not further investigate the meiotic defect of *cnm67Δ1* strains, and it is probable that *Cnm67p* is also critical for meiotic spindle orientation. The sporulation deficiency cannot be due to the multinucleate phenotype per se since about 60% of *cnm67Δ1* cells contain only one nucleus. We

might also expect that cells with a reduced outer plaque would have less pronounced defects in nuclear congression during mating as compared with nuclear migration in mitosis, since cytoplasmic microtubules are organized by the half-bridge during mating (Byers and Goetsch, 1975). This is exactly what we observed for *cnm67Δ1* strains as nuclear congression is not significantly impaired, although orientation of mitotic spindles is clearly inefficient. *In vivo* observation of nuclei during conjugation allowed us to conclude that kinetics of nuclear congression and fusion are normal in *cnm67Δ1* cells. The observed reduced frequency of diploid formation is due to a substantial number of mating cells carrying more than one nucleus and to frequent mitotic missegregation of diploid nuclei.

The apparent reduction of the outer plaque in *cnm67Δ1* mutants raises the question of how cells manage to keep a partial nuclear migration capability during mitosis as orientation of the nucleus within the cell and movement through the bud neck are strictly dependent on the function of cytoplasmic microtubules (Huffaker *et al*., 1988; Palmer *et al*., 1992; Sullivan and Huffaker, 1992), and yet immunofluorescence of *cnm67Δ1* cells clearly shows the presence of cytoplasmic microtubules. In addition, these microtubules in cells with misoriented spindles are often directed into the bud, suggesting that factors controlling overall microtubule directionality are at least partially functional. Examination of *cnm67Δ1* SPBs by serial thin section electron microscopy indicated that cytoplasmic microtubules fail to transfer to the outer plaque after SPB separation as in wild-type cells (Byers and Goetsch, 1975), but remain attached to the half-bridge throughout the cell cycle. Presumably, this interaction allows motor proteins to generate pulling or pushing forces that, to a certain extent, position the nucleus and thus allow cells to propagate, although force transfer to the SPB is less efficient than in cells with cytoplasmic microtubules attached to the outer plaque.

Since *cnm67Δ1* cells have cytoplasmic microtubules, why then is nuclear migration less efficient in the mutant? It seems possible that different motor proteins act on microtubules initiated from the SPB outer plaque compared with those from the half-bridge. Thus, a motor protein might function less efficiently if the microtubules were attached to an inappropriate structure for that particular stage of the cell cycle, which might change the dynamic behavior of the microtubules (Carminati and Stearns, 1997; Shaw *et al*., 1997). Interestingly, DeZwaan *et al*. (1997) recently found that the kinesin-related motor Kip3p predominantly acts in the first phase of nuclear migration whereas dynein mainly contributes to the second phase. During the first, Kip3p mediated- phase microtubules are presumably attached at the half-bridge or bridge whereas they are organized by the outer plaque during the second, dynein-mediated phase. Cottingham and Hoyt (1997) demonstrated the involvement of yet another kinesin-related protein, Kip2p, in proper spindle positioning. Future studies may reveal how different motor protein functions relate to differential attachment of cytoplasmic microtubules to different SPB substructures.

ACKNOWLEDGMENTS

We are grateful to Douglas Kershaw for cutting the serial thin sections for EM and to Dominic Hoepfner and Florian Schärer for help with construction of the Hhf2-GFPp-labeled strains and software development. We also thank M.N. Hall, W.D. Heyer, I. Adams, and S. Souès for discussion. A. Duesterhoeft is gratefully acknowledged for providing sequence information and subclones of cosmid XIV-6. Thanks are also due to D. Botstein, J. Cooper, and D. Koshland for strains. This work was supported by grants to P.P. and A.W. from the Swiss Federal office for Education and Science (grants 95.0191–1 and 95.0191–12).

REFERENCES

Adams, A.E., and Pringle, J.R. (1984) Relationship of actin and tubulin distribution to bud growth in wild-type and morphogenetic-mutant *Saccharomyces cerevisiae*. J. Cell Biol. *98*, 934–945.

Berger, B., Wilson, D.B., Wolf, E., Tonchev, T., Milla, M., and Kim, P.S. (1995). Predicting coiled coils by use of pairwise residue correlations. Proc. Natl. Acad. Sci. USA *92*, 8259–8263.

Baudin, A., Ozier, K.O., Denouel, A., Lacroute, F., and Cullin, C. (1993). A simple and efficient method for direct gene deletion in *Saccharomyces cerevisiae*. Nucleic Acids Res. *21*, 3329–3330.

Brinkley, B.R. (1985). Microtubule organizing centers. Annu. Rev. Cell Biol. *1*, 145–172.

Bullitt, E., Rout, M.P., Kilmartin, J.V., and Akey, C.W. (1997). The yeast spindle pole body is assembled around a central crystal of Spc42p. Cell *89*, 1077–1086.

Bullock, W.O., Fernandez, J.M., and Short, J.M. (1987). XLl-Blue: a high efficiency plasmid transforming recA *Escherichia coli* strain with $^{\beta}$-galactosidase selection. BioTechniques *5*, 376–378.

Byers, B. (1981). Cytology of the yeast life cycle. In: The Molecular Biology of the Yeast *Saccharomyces*-Life Cycle and Inheritance, ed. J.N. Strathern, J.N., E.W. Jones, and J.R. Broach, Cold Spring Harbor, NY: Cold Spring Harbor Laboratory, 59–96.

Byers, B., and Goetsch, L. (1975). Behavior of spindles and spindle plaques in the cell cycle and conjugation of *Saccharomyces cerevisiae*. J. Bacteriol. *124*, 511–523.

Byers, B., and Goetsch, L. (1991). Preparation of yeast cells for thin section electron microscopy. Methods Enzymol. *194*, 602–607.

Carminati, J.L., and Stearns, T. (1997). Microtubules orient the mitotic spindle through dynein-dependent interactions with the cell cortex. J. Cell Biol. *138*, 629–641.

Clark, S.W., and Meyer, D.I. (1994). ACT3: a putative centractin homologue in *S. cerevisiae* is required for proper orientation of the mitotic spindle. J. Cell Biol. *127*, 129–138.

Cottingham, F.R., and Hoyt, M.A. (1997). Mitotic spindle positioning in *Saccharomyces cerevisiae* is accomplished by antagonistically acting microtubule motor proteins. J. Cell Biol. *138*, 1041–1053.

Cross, F., Hartwell, L.H., Jackson, C., and Konopka, J.B. (1988). Conjugation in *Saccharomyces cerevisiae.* Annu. Rev. Cell Biol., *44*, 29–57.

Delgado, M.A., and Conde, J. (1984). Benomyl prevents nuclear fusion in *Saccharomyces cerevisiae*. Mol. Gen. Genet. *193*, 188–189.

DeZwaan, T.M., Ellingson, E., Pellman, D., and Roof, D.M. (1997). Kinesin related *KIP3* of *Saccharomyces cerevisiae* is required for a distinct step of nuclear migration. J. Cell Biol. *138*, 1023–1040.

Eshel, D., Urrestarazu, L.A., Vissers, S., Jauniaux, J.C., van Vliet-Reedijk, J.C., Planta, R.J., and Gibbons, I.R. (1993). Cytoplasmic dynein is required for normal nuclear segregation in yeast. Proc. Natl. Acad. Sci. USA *90*, 11172–11176.

Freifelder, D. (1960) Bud formation in *Saccharomyces cerevisiae*. J. Bacteriol., *80*, 567–568.

Geissler, S., Pereira, G., Spang, A., Knop, M., Soues, S., Kilmartin, J.V., and Schiebel, E. (1996). The spindle pole body component Spc98p interacts with the gamma-tubulin-like Tub4p of *Saccharomyces cerevisiae* at the sites of microtubule attachment. EMBO J. *15*, 3899–3911.

Goh, P.-Y., and Kilmartin, J.V. (1993). NDC10: a gene involved in chromosome segregation in *Saccharomyces cerevisiae*. J. Cell Biol., *121*, 503–512.

Guthrie, C., and Fink, G.R. (1991). Guide to yeast genetics and molecular biology. Methods Enzymol. *194*, 14–15.

Haarer, B.K., Lillie, S.H., Adams, A.E., Magdolen, V., Bandlow, W., and Brown, S.S. (1990). Purification of profilin from *Saccharomyces cerevisiae* and analysis of profilin-deficient cells. J. Cell Biol. *110*, 105–114.

Hasek, J., Rupes, I., Svobodova, J., Streiblova, E. (1987). Tubulin and actin topology during zygote formation of *Saccharomyces cerevisiae*. J. Gen. Microbiol. *133*: 3355–63.

Hoyt, M.A., Totis, L., and Roberts, B.T. (1991). S. cerevisiae genes required for cell cycle arrest in response to loss of microtubule function. Cell *66*, 507–517.

Huffaker, T.C., Thomas, J.H., and Botstein, D. (1988). Diverse effects of beta-tubulin mutations on microtubule formation and function. J. Cell Biol. *106*, 1997–2010.

Horesh, O., Simchen, G., and Friedmann, A. (1979). Morphogenesis of the synapton during yeast meiosis. Chromosoma *75*, 101–115.

Huxley, C., Green, E.D., and Dunham, I. (1990). Rapid assessment of *S. cerevisiae* mating type by PCR. Trends Genet. *6*, 236.

Interthal, H., Bellocq, C., Bahler, J., Bashkirov, V.I., Edelstein, S., and Heyer, W.D. (1995). A role of Sep1 (= Kem1, Xrn1) as a microtubule-associated protein in *Saccharomyces cerevisiae*. EMBO J. *14*, 1057–1066.

Kalt, A., and Schliwa, M. (1996). A novel structural component of the Dictyostelium centrosome. J. Cell Sci. *109*, 3103–3112.

Kellogg, D.R., Moritz, M., and Alberts, B.M. (1994) The centrosome and cellular organization. Annu. Rev. Biochem. *63*, 639–674.

Kilmartin, J.V., and Adams, A.E. (1984). Structural rearrangements of tubulin and actin during the cell cycle of the yeast *Saccharomyces*. J. Cell Biol. *98*, 922–933.

Kilmartin, J.V., Dyos, S.L., Kershaw, D., and Finch, J.T. (1993). A spacer protein in the *Saccharomyces cerevisiae* spindle poly body whose transcript is cell cycle-regulated. J. Cell Biol. *123*, 1175–1184.

Kilmartin, J.V. (1994). Genetic and biochemical approaches to spindle function and chromosome segregation in eukaryotic microorganisms. Curr. Opin. Cell Biol. *6*, 50–54.

Knop, M., Pereira, G., Geissler, S., Grein, K., and Schiebel, E. (1997). The spindle pole body component Spc97p interacts with the gamma-tubulin of *Saccharomyces cerevisiae* and functions in microtubule organization and spindle pole body duplication. EMBO J. *16*, 1550–1564.

Kurihara, L.J., Beh, C.T., Latterich, M., Schekman, R., and Rose, M.D. (1994). Nuclear congression and membrane fusion: two distinct events in the yeast karyogamy pathway. J. Cell Biol. *126*, 911–923.

Li, R., and Murray, A.W. (1991). Feedback control of mitosis in budding yeast. Cell *66*, 519–531.

Li, Y.Y., Yeh, E., Hays, T., and Bloom, K. (1993). Disruption of mitotic spindle orientation in a yeast dynein mutant. Proc. Natl. Acad. Sci. USA *90*, 10096–10100.

Magdolen, V., Oechsner, U., Muller, G., and Bandlow, W. (1988). The intron-containing gene for yeast profilin (*PFY*) encodes a vital function. Mol. Cell. Biol. *8*, 5108–5115.

Marschall, L.G., Jeng, R.L., Mulholland, J., and Stearns, T. (1996) Analysis of Tub4p, a yeast gamma-tubulin-like protein: implications for microtubule-organizing center function. J. Cell Biol. *134*, 443–454.

McElver, J., and Weber, S. (1992). Flag N-terminal epitope overexpression of bacterial alkaline phosphatase and Flag C-terminal epitope tagging by PCR one-step targeted integration. Yeast *8* (special issue), 627.

McMillan, J.N., and Tatchell, K. (1994). The *JNM1* gene in the yeast *Saccharomyces cerevisiae* is required for nuclear migration and spindle orientation during the mitotic cell cycle. J. Cell Biol. *125*, 143–158.

Moens, P.B., and Rapport, E. (1971). Spindles, spindle plaques, and meiosis in the yeast *Saccharomyces cerevisiae* (Hansen). J. Cell Biol. *50*, 344–361.

Muhua, L., Karpova, T.S., and Cooper, J.A. (1994). A yeast actin-related protein homologous to that in vertebrate dynactin complex is important for spindle orientation and nuclear migration. Cell *78*, 669–679.

Palmer, R.E., Sullivan, D.S., Huffaker, T., and Koshland, D. (1992). Role of astral microtubules and actin in spindle orientation and migration in the budding yeast, *Saccharomyces cerevisiae*. J. Cell Biol. *119*, 583–593.

Pearson, W.R., and Lipman, D.J. (1988). Improved tools for biological sequence comparison. Proc. Natl. Acad. Sci. USA *85*, 2444–2448.

Pereira, G., and Schiebel, E. (1997) Centrosome-microtubule nucleation. J. Cell Sci. *110*, 295–300.

Philippsen, P. *et al*. (1997). The nucleotide sequence of *Saccharomyces cerevisiae* chromosome XIV and its evolutionary implications. Nature *387* (suppl), 93–98.

Rose, M.D. (1996). Nuclear fusion in the yeast *Saccharomyces cerevisiae*. Annu. Rev. Cell Biol. *12*, 663–695.

Rose, M.D., Biggins, S., and Satterwhite, L.L. (1993) Unravelling the tangled web at the microtubule-organizing center. Curr. Opin. Cell Biol. *5*, 105–115.

Rose, M.D., and Fink, G.R. (1987). KAR1, a gene required for function of both intranuclear and extranuclear microtubules in yeast. Cell *48*, 1047–1060.

Rout, M.P., and Kilmartin, J.V. (1990). Components of the yeast spindle and spindle pole body. J. Cell Biol. *111*, 1913–1927.

Sambrook, J., Fritsch, E.F., and Maniatis, T. (1989). Molecular Cloning: A Laboratory Manual, 2nd ed., Cold Spring Harbor, NY: Cold Spring Harbor Laboratory Press.

Schiestl, R.H., and Gietz, R.D. (1989). High efficiency transformation of intact yeast cells using single stranded nucleic acids as a carrier. Curr. Genet. *16*, 339–346.

Schutz, A.R., Giddings, T.H., Steiner, E., and Winey, M. (1997). The yeast *CDC37* gene interacts with *MPS1* and is required for proper execution of spindle pole body duplication. J. Cell Biol. *136*, 969–982.

Shaw, S.L., Yeh, E., Maddox, P., Salmon, E.D., and Bloom, K. (1997). Astral microtubule dynamics in yeast: a microtubule-based searching mechanism for spindle orientation and nuclear migration into the bud. J. Cell Biol. *139*, 985–994.

Sikorski, R.S., and Hieter, P. (1989). A system of shuttle vectors and yeast host strains designed for efficient manipulation of DNA in *Saccharomyces cerevisiae*. Genetics *122*, 19–27.

Snyder, M. (1994). The spindle pole body of yeast. Chromosoma *103*: 369–380.

Sobel, S.G., and Synder, M. (1995). A highly divergent gamma-tubulin gene is essential for cell growth and proper microtubule organization in *Saccharomyces cerevisiae*. J. Cell Biol. *131*, 1775–1788.

Solomon, F. (1991). Analyses of the cytoskeleton in *Saccharomyces cerevisiae*. Annu. Rev. Cell Biol. 633–662.

Spang, A., Geissler, S., Grein, K., and Schiebel, E. (1996). gamma-Tubulin-like Tub4p of *Saccharomyces cerevisiae* is associated with the spindle pole body substructures that organize microtubules and is required for mitotic spindle formation. J. Cell Biol. *134*, 429–441.

Stearns, T., Hoyt, M.A., and Botstein, D. (1990). Yeast mutants sensitive to antimicrotubule drugs define three genes that affect microtubule function. Genetics *124*, 251–262.

Sullivan, D.S., and Huffaker, T.C. (1992). Astral microtubules are not required for anaphase B in *Saccharomyces cerevisiae*. J. Cell Biol. *119*, 379–388.

Thomas, J.H., Neff, N.F., and Botstein, D. (1985). Isolation and characterization of mutations in the beta-tubulin gene of *Saccharomyces cerevisiae*. Genetics *111*, 715–734.

Wach, A., Brachat, A., Pöhlmann, R., and Philippsen, P. (1994). New heterologous modules for classical or PCR-based gene disruptions in *Saccharomyces cerevisiae*. Yeast *10*, 1793–1808.

Wach, A., Brachat, A., Alberti-Segui, C., Rebischung, C., and Philippsen, P. (1997). Heterologous *HIS3* marker and GFP reporter modules for *Saccharomyces cerevisiae* transformation with SFH-PCR products. Yeast *13*, 1065–1075.

Weiss, E., and Winey, M. (1996). The *Saccharomyces cerevisiae* spindle pole body duplication gene *MPS1* is part of a mitotic checkpoint. J. Cell Biol. *132*, 111–123.

Winey, M., and Byers, B. (1993). Assembly and functions of the spindle pole body in budding yeast. Trends Genet. *9*, 300–304.

Yeh, E., Skibbens, R.V., Cheng, J.W., Salmon, E.D., and Bloom, K. (1995). Spindle dynamics and cell cycle regulation of dynein in the budding yeast, *Saccharomyces cerevisiae*. J. Cell Biol. *130*, 687–700.